Thermally Stimulated Current and Dielectric Studies of Poly(aryl ether ketone ketone)

Bryan B. Sauer,*,† Peter Avakian,† Howard W. Starkweather, Jr.,† and Ben S. Hsiao‡

E. I. du Pont de Nemours and Company, Inc., Central Research and Development and Fibers Departments, Experimental Station, Wilmington, Delaware 19898

Received February 2, 1990; Revised Manuscript Received May 18, 1990

ABSTRACT: Thermally stimulated current depolarization (TSC), dielectric, and differential scanning calorimetry (DSC) techniques were used to study crystallization and molecular relaxations in poly(aryl ether ketone ketone) (PEKK). The α relaxation, associated with the glass transition (T_g = 155 °C), was studied with TSC before and after crystallization, showing that crystallinity substantially hinders amorphous relaxations, consistent with DSC analysis of the glass transition. Thermal peak cleaning was used to deconvolute the global TSC spectra, giving apparent activation energies E_a over the range −120 to +240 °C. Comparison of analysis schemes to obtain activation energies either by numerical integration or by fit of the raw TSC spectra in current space is discussed. The mean values of E_a from thermally cleaned TSC spectra were in agreement with those determined from classical Arrhenius plots of the dielectric α and β relaxation data of ln f versus $1/T_{max}$, where T_{max} is the peak temperature. TSC has the advantage that values of E_a can be determined at any temperature regardless of whether a specific transition is present. In the sub-T_g region from −120 to 130 °C, the activation energy increased gradually with temperature and the values of E_a were found to agree quantitatively with those predicted by using Eyring's activated states equation with a zero activation entropy. The activation energies for both amorphous and semicrystalline PEKK were found to be identical over the range covered. At higher temperatures, the measured values of E_a depart from the zero activation entropy line and exhibit a sharp maximum at T_g, indicating a high degree of cooperativity in the relaxations.

Introduction

Relaxations in semicrystalline polymers mediate properties such as modulus and toughness. There are difficulties in interpretation of relaxation dynamics because of the complexity of solid-state polymers and also because conflicting results are sometimes obtained by different techniques such as dielectric, mechanical, and NMR.[1] These differences may reflect differing sensitivity to structural features such as dipoles in the case of dielectric or to more macroscopic types of structures in the case of dynamical mechanical. Other discrepancies are attributable to the various techniques sampling different relaxation distributions due to the different frequencies and probe length scales of the techniques. To improve our understanding of relaxation dynamics, we have chosen to compare results from TSC and conventional ac dielectric techniques, which when used together, cover a wide frequency range. A favorable comparison would serve to substantiate the TSC technique and also advance our understanding of some of the more subtle features of dielectric relaxations on a molecular scale and their thermodynamic basis.

The influence of crystal morphology on the motion of amorphous segments has been reviewed.[1,2] It has been proposed that, for small crystallite dimensions, the crystallites act as cross-links in a network inhibiting the movement of the segments in the amorphous regions. For larger crystallites, the material in the amorphous regions is generally less affected. Crystallite dimensions and the resulting polymer properties are determined mainly by thermal history during and after processing. In the case of PEKK, crystal growth can be initiated either directly from the melt or by quenching below T_g followed by annealing above T_g. The latter process is termed cold crystallization and is usually dominated by nucleation processes, giving rather small spherulite dimensions with a high number density. This paper deals with both amorphous and cold-crystallized samples. For PEKK, as with poly(aryl ether ether ketone) (PEEK), DSC[3] and TSC indicate that the maximum crystallinity can be reached within minutes at temperatures 10's of degrees above T_g.

The TSC technique (sometimes referred to as thermally stimulated dielectric relaxation) is highly sensitive and gives reproducible results in terms of polymer transitions, as is indicated by several review articles.[4-6] The low equivalent frequency[4] of TSC ($\sim 10^{-4}$–10^{-2} Hz) leads to enhanced resolution of the different relaxation processes, allowing direct comparison with DSC in terms of viscoelastic relaxations such as the glass transition (or α transition). Other more complicated transitions due to injected space charges, charge trapping at crystal interfaces, and crystal growth have been detected by this techniques.[4,7] One disadvantage of classical ac dielectric techniques is that the relatively high probe frequencies (1–10^{12} Hz) cause the various transitions due to molecular motions to merge at higher frequencies.[1] Other complications occur when dealing with crystallizable polymers because the α relaxation shifts to higher temperatures with increasing frequency. Because of this, when one attempts to study the α relaxation in amorphous PEKK or PEEK, using dynamical mechanical or ac dielectric at frequencies above a few hertz, the sample crystallizes during the measurement. Due to its low equivalent frequency, TSC is quite useful for the study of the α relaxation in amorphous materials such as PEKK and PEEK. In some materials crystallization is slow enough so that the pure amorphous material can be readily studied with ac dielectric methods without significant crystallization. For example, in the case of poly(ethylene terephthalate) it has been shown that the α relaxation is substantially broader in the semicrystalline material than that in the purely amorphous material.[1,2]

Several TSC reports have illustrated the advantages of the programmable nature of the initial polarization, which allows one to excite only the specific transition of interest. Thermal peak cleaning (or windowing polarization) of the

† Central Research and Development Department.
‡ Fibers Department.

0024-9297/90/2223-5119$02.50/0

TSC global spectra has been used to pursue the underlying mechanisms responsible for broad or structured relaxation peaks, especially in low-temperature secondary relaxations.[6,8] Analysis of the relaxation dynamics by thermal peak cleaning has led to only marginal accuracy to date with reported values of E_a considerably lower than those extracted from ac dielectric or mechanical methods.[8,9] For some low-temperature transitions, such as those in oxidized polyethylene, it was shown that E_a determined by TSC compares well with that determined by other techniques.[10,11] Improvements in instrumentation and careful characterization of dynamics using complementary techniques such as TSC and ac dielectric measurements on the same sample have allowed us to obtain a more complete picture of the temperature dependence of relaxations. We have found excellent agreement of E_a obtained by thermal cleaning of the TSC spectra with those activation energies determined by dielectric and dynamical mechanical measurements, not only for low-temperature transitions but also for higher temperature ones such as the glass transition.

For an individual thermally cleaned TSC spectrum, some questions remain as to the breadth of the relaxation. Various schemes were tested for the analysis of the thermally cleaned spectra, which indicated that the mean values of E_a obtained by the Bucci method[12] using numerical integration of the thermally cleaned TSC current peak and those calculated by fitting the explicit relationship developed by Fröhlich[11,13] for the current were equivalent. The parameters obtained by the Fröhlich method suggest that the distribution of relaxations in terms of a distribution of activation energies is extremely narrow for the low-temperature secondary relaxations.

Experimental Section

Materials and Sample Preparation. The chosen PEKK was a copolymer of diphenyl ether, terephthalyl chloride, and isophthalyl chloride and has the chemical repeat unit indicated below.

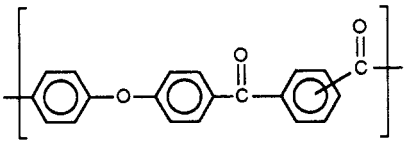

In this structure the diagonal line indicates that this material is a copolymer of terephthalyl (para) and isophthalyl (meta) ketone linkages. The PEKK studied here is the same as that reported earlier[14] and has T_g = 156 °C and a crystal melting temperature of about 338 °C measured at 10 °C/min by DSC (Figure 1). The crystal melting temperature depends on thermal history. The weight-average molecular weight determined by GPC with polystyrene standards is approximately 30 000 g/mol. The thermal behavior of PEKK is similar to that of PEEK, with PEEK having a lower T_g and about the same crystal melting temperature as measured by DSC.[3,14]

Amorphous PEKK films were prepared by pressing a pellet on a hot plate at ~360 °C, holding for several seconds to eliminate crystallinity, and then quenching at approximately 100 °C/s. PEKK films were stored under vacuum (10^{-4}–10^{-5} mbar) at 30 °C. Films were between 0.05 and 0.11 mm thick with areas of ~50 mm². The film was confined between parallel plates, with the upper plate spring-loaded to maintain electrical contact as the film underwent minor thermal expansion and contraction during thermal cycling. Further improvements in electrode contact were made by sputter coating both sides of the film with gold. This was only important for the very weak low-temperature β transition (currents on the order of 10^{-14} A). Some low-temperature results were obtained by painting a small piece of film (10 mm × 10 mm × 0.1 mm) with colloidal silver and attaching wires. The sample was suspended next to the thermister in the cell to obtain accurate temperature values. The silver electrodes could not be used above ~180 °C because of decomposition.

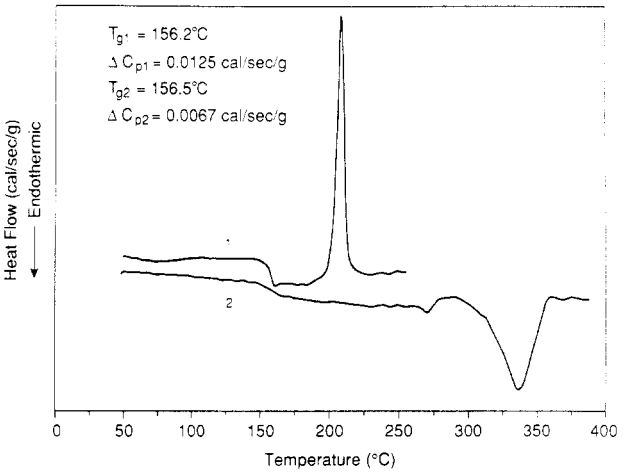

Figure 1. DSC heat flow vs temperature for amorphous PEKK (first run) and semicrystalline PEKK (second run).

Characterization Techniques. A Du Pont differential scanning calorimeter (Model 910) coupled to a 9900 thermal analysis system was used to characterize the thermal behavior of PEKK. The heating rate in dry nitrogen was 10 °C/min.

The ac dielectric experiments were done by using the parallel-plate geometry with sputter-coated polymer films. A Hewlett Packard LCR meter (Model 4274A) was used to measure the capacitance, C, and dissipation factor ($\tan\delta = \epsilon''/\epsilon'$) of the sample at 11 frequencies in the range 10^2–10^5 Hz from −190 °C < T < 250 °C at a heating rate of 1.5 °C/min. The data were stored in a Hewlett Packard personal computer. The real ϵ' and imaginary ϵ'' components of the dielectric constant (or dielectric permittivity) were calculated by using

$$\epsilon' = dC/(\epsilon_0 A), \quad \epsilon'' = \epsilon' \tan\delta \tag{1}$$

where d is the sample thickness, ϵ_0 the permittivity of vacuum (8.854×10^{-12} F/m), A the metallized electrode area (350 mm²), and δ the loss angle.

A TSC spectrometer (Solomat Instruments, Stamford, CT) was used covering the temperature range −180 to +300 °C. A Faraday cage shields the sample, and prior to the experiment the sample cell is evacuated to ~10^{-4} mbar and subsequently flushed several times with 1.1 bar of high-purity He (Grade 5.5, 99.9995%, Keen compressed gas).

Two different methods of polarizing the sample were used to obtain "global" TSC spectra or thermally cleaned TSC spectra.

Method 1. For global spectra the film was first polarized by a static electric field (E ~ 100–2000 kV/m) at the polarization temperature T_p for 2 min and then quenched down to the "freezing temperature" T_0, with cooling during polarization at approximately 20 °C/min to freeze in dipolar orientation. With the field turned off and the sample short circuited, the depolarization current due to dipolar reorientation was measured as the temperature was increased from T_0 at 7 °C/min to the final temperature T_f ($\geq T_p$).

Method 2. Thermal cleaning was performed by applying the polarization field (E ~ 100–2000 kV/m) during the following thermal cycles: 2 min at T_p, quenching to T_p −5 °C, and holding for 2 min more. The field is then removed, and the sample is quenched 40 °C below this polarization temperature window. The depolarization spectrum due to a narrow distribution of relaxations was then measured upon heating at 7 °C/min to temperatures about 30 °C above T_p.

The global TSC is a convoluted spectrum of all dielectrically active relaxations excited between T_p and T_0. Equation 2 gives the relationship of the change in polarization, ΔP, to the change in dielectric constant, $\Delta\epsilon$, for the sum of the processes over the temperature and frequency range covered. Experimentally, one can determine $\Delta\epsilon$ by integrating the area under the TSC curve[4,15]

$$\Delta P = \epsilon_0 \Delta\epsilon E = \int_{t_0}^{\infty} j \, dt \quad (2)$$

where E is the polarizing field strength in V/m, t_0 is the time at which the depolarization scan was started, and the current density ($j = J/A$) is defined as the measured current, J, divided by the area of the sample, A, in contact with the electrode.

van Turnhout[4] has shown that the global TSC is equivalent to a low-frequency dielectric loss experiment with

$$\epsilon''(f) = J(t)/(\epsilon_0 A 2\pi f E) \quad (3)$$

where f is the equivalent frequency of the TSC experiment defined by

$$f = E_a/(2\pi s R T^2) \quad (4)$$

Here s is the inverse heating rate ($(7\ °C/min)^{-1} = 8.57\ s/°C$), and $R = 1.987$ cal K^{-1} mol^{-1} is the ideal gas constant.

Various methods have been used to analyze the thermally cleaned TSC spectra. Bucci et al.[12] have proposed that the relaxation time, $\tau(T)$, is related to the measured depolarization current, $J(T)$, by

$$\ln \tau(T) = \ln \{ \int_{T_0}^{T} J(T)\, dT \} - \ln J(T) \quad (5)$$

where the polarization is defined as

$$P(T) = \int_{T_0}^{T} J(T)\, dT \quad (6)$$

and T_0 is the initial temperature of the depolarization scan. They assumed that the relaxation time constant τ is related to the barrier height or apparent activation energy, E_a, in the Arrhenius equation

$$\tau(T) = \tau_0 \exp(E_a/RT) \quad (7)$$

where τ_0 is the preexponential factor. The integral of J is evaluated numerically, and the values of $\tau(T)$, typically spanning the range $10^1\ s < \tau < 10^4$ s, are plotted versus reciprocal temperature in a Bucci plot.[12] In many cases a linear dependence of $\ln \tau$ on $1/T$ is found[6,11] with the slope equal to $E_a/1.987$ if E_a is in calories per mole.

The second method of evaluating the thermally cleaned spectra, which we will refer to as the "Fröhlich method",[13] allows one to fit the measured current directly by using[11,12]

$$J(T) = P_0/\tau_0 \exp\{-E_a/RT - s/\tau_0 \int_{T_0}^{T} \exp(-E_a/RT')\, dT' \} \quad (8)$$

Here P_0 is a constant related to the polarization. The integral in eq 8 can be approximated as[16,17]

$$\int_{T_0}^{T} \exp\left(-\frac{E_a}{RT'}\right) dT' = \left. \frac{T' \exp(-x)(x + 3.0396)}{(x^2 + 5.0364x + 4.1916)} \right|_{T'=T_0}^{T'=T} \quad (9)$$

where x is defined as E_a/RT. Equation 8 is a rapidly changing function, which, unlike experiment, predicts a spectrum that is quite asymmetric as a function of temperature. One can generate symmetric spectra by assuming a Gaussian distribution of relaxations as in[12,17]

$$J(T) = \int_0^{\infty} \exp[-(E_a - E_{a,0})^2/2\sigma^2] J(T,E_a)\, dE_a \quad (10)$$

where $E_{a,0}$ is the mean activation energy and σ is the width of the Gaussian distribution. Surprisingly, one can also generate symmetric TSC spectra by assuming discrete values of E_a

$$J(T) = \sum_{i=1}^{3} a_i J(T,E_{a,i}) \quad (11)$$

where a_i is the amplitude corresponding to the ith activation energy $E_{a,i}$ and J is calculated by using eq 8. We have found that, in general, assuming three discrete values of E_a with a distribution less than $\pm 0.03 E_a$ results in a relatively symmetric peak that fits the data.

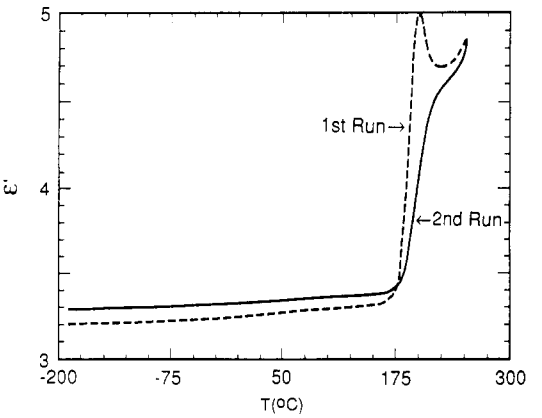

Figure 2. Dielectric constant ϵ' vs temperature at 1 kHz for the first and second temperature scans on PEKK. During the first run the sample is cold crystallized resulted in a peak at 205 °C. The second run is for a semicrystalline (~27%) sample.

It has been suggested that there is more than 1 order of magnitude discrepancy[11] between the Fröhlich (eq 10) and the Bucci (eq 5) methods of analysis. We will show in this report that mean values of E_a determined by the two methods agree within a few percent. There are advantages of estimating the distribution by fitting the current directly using the Fröhlich method, because the Bucci analysis is rather insensitive to the presence of distributed relaxations.[11]

Results and Discussion

Thermal Analysis. DSC heating scans at 10 °C/min are given in Figure 1 for amorphous (aPEKK) and semicrystalline (cPEKK) films. The amorphous PEKK films used for DSC and TSC were formed by quenching from 360 °C at a rate of ~100 °C/s. Figure 1 indicates that T_g = 156 °C for aPEKK and a large exothermic change is also detected with a maximum at 207 °C as cold crystallization takes place. T_g also occurs at 156 °C for the second heating, and the transition is significantly broadened. The magnitude of the heat capacity change at the glass transition for cPEKK is a factor of 2 ± 0.5 smaller than that for aPEKK. The heat of fusion determined by integrating the endothermic melting peak at ~330 °C for the second run was 34 ± 2 J/g indicating that approximately 27% crystallinity had developed which is comparable to that measured by other techniques.[14,18,19] This estimate is based on the assumption that PEKK is the same as PEEK in terms of the heat of fusion, which is about 130 J/g for PEEK crystals.[3,20] A second smaller endothermic transition peak appears at 270 °C, which is ~10 °C above the annealing temperature for the first run. This phenomenon has been observed in other polymers[3,21] and has been referred to as double melting behavior.

Dielectric Spectra. The real part of the dielectric constant ϵ' at 1 kHz is plotted versus T in Figure 2 for the first and second runs on an originally amorphous sample of PEKK. There is a large difference due to crystallization that influences the first run starting at temperatures above 170 °C. This produces an "artificial" maximum in ϵ' at 205 °C as the growing crystals reduce segmental mobility. The maximum at 205 °C is superimposed on the glass transition (or α) peak, which is shifted from the DSC T_g of 156 to ~200 °C (at 10 kHz) due to the high frequency, making it impossible to study the glass transition in purely amorphous PEKK by this technique. At the end of the first run in Figure 2, the cold crystallization is essentially complete and no further changes occur during the second run, as is indicated by the continuously increasing curve with no crystal growth peak. The α transition for the second run is readily examined by plotting the dissipation

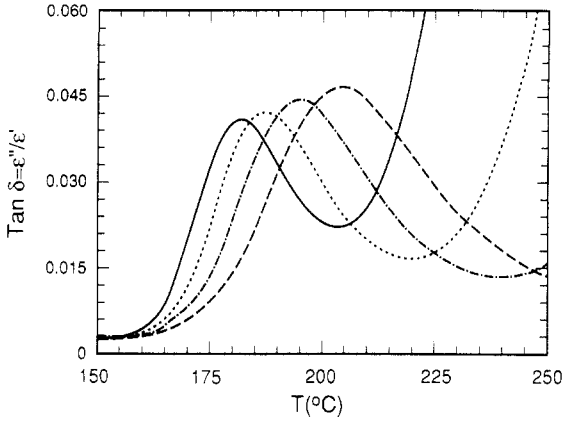

Figure 3. Frequency dependence of the dissipation factor tan $\delta = \epsilon''/\epsilon'$ vs temperature for the α transition at 0.1 kHz (solid line), 1 kHz (short dashes), 10 kHz (dot-dash), and 100 kHz (long dashed line) for semicrystalline (~27%) PEKK.

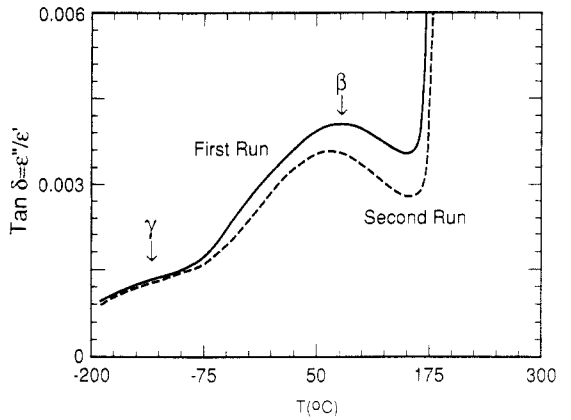

Figure 4. tan $\delta = \epsilon''/\epsilon'$ plotted for the ac dielectric β and γ transitions at 1 kHz for the first and second runs on PEKK.

factor (ϵ''/ϵ') versus T (Figure 3). The activation energy of the transition governs the amount that the peak temperature (T_{max}) shifts with frequency. Conductivity contributes to the strong upturn at the highest temperatures in Figure 3, and this is also frequency dependent, becoming almost negligible at 100 kHz. We do not present the frequency dependence in the α region for aPEKK because it is masked by crystal growth.

Figure 4 is an expanded view of the low-temperature region of the γ and β relaxations in terms of ϵ''/ϵ' at 1 kHz for both aPEKK and cPEKK. The γ relaxation at −135 °C is independent of crystallinity, and the β relaxation at ~70 °C is reduced by ~25% in magnitude for cPEKK as compared to that for aPEKK. Thus, the relaxation strength is reduced by an amount proportional to the degree of crystallinity, consistent with the idea that the β transition is due to local segmental motions uninfluenced by neighboring crystallites.

Figure 5 is a plot of the frequency dependence of ϵ''/ϵ' for the β relaxation in cPEKK. There is a strong frequency dependence of T_{max} due to the low value of E_a, and the β transition merges with the α transition at 100 kHz.

From data at different frequencies, log f vs $1/T_{max}$ Arrhenius relaxation maps[1] are constructed. The TSC peak temperatures are included corresponding to equivalent frequencies calculated by using eq 4. The slope is proportional to E_a in these plots. It is evident that the TSC data are consistent with the dielectric data for the β transition in Figure 6, but there is systematic curvature in the dielectric data in Figure 7 for α. The activation energies calculated from least-squares fits are E_a = 13.8 ± 0.5 kcal/mol for β and E_a = 139 ± 10 kcal/mol for α, and both of these values agree with those obtained by thermal peak cleaning of the TSC spectra, as will be discussed later. The deviation from simple Arrhenius behavior such as that in Figure 7 is a common occurrence for α relaxations.[1] Because of the deviation, the calculated activation energy is only a rough estimate, and the results are analyzed in terms free volume concepts using the empirical WLF equation[1,22]

$$\log(\tau/\tau_0) = \log(f_0/f) = -C_1(T - T_0)/[C_2 + (T - T_0)] \quad (12)$$

where C_1 and C_2 are material constants, and T_0 is set equal

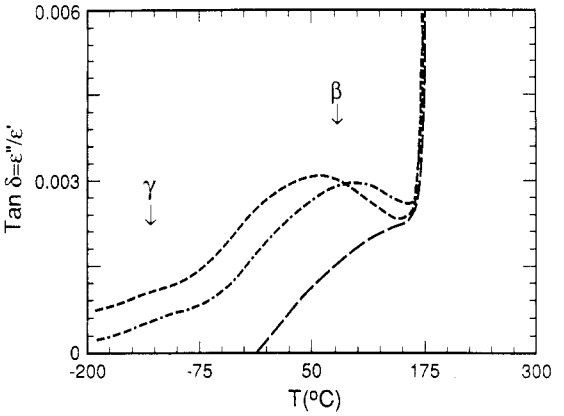

Figure 5. Frequency dependence of tan $\delta = \epsilon''/\epsilon'$ vs temperature for the β relaxation at 1 kHz (short dashed line), 10 kHz (dot-dash), and 100 kHz (long dashed line) for semicrystalline (second run) PEKK. The downward base-line shift at 100 kHz is an instrumental artifact and is not due to the sample.

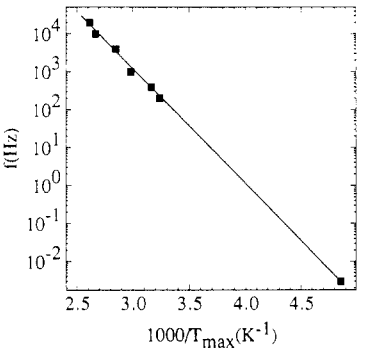

Figure 6. Arrhenius plot of log f vs the reciprocal peak temperature, $1/T_{max}$, for the β relaxation in PEKK for both TSC (0.003 Hz) and dielectric data. The slope gives an activation energy of 13.8 ± 0.2 kcal/mol.

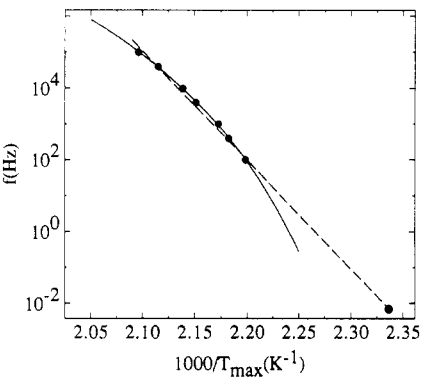

Figure 7. Arrhenius plot of log f vs the reciprocal peak temperature, $1/T_{max}$, for the α relaxation in PEKK for both TSC (0.007 Hz) and dielectric data. The slope of the Arrhenius fit (dashed line) gives an activation energy of 139 kcal/mol. The solid curve is a WLF fit to the high-frequency data (see text).

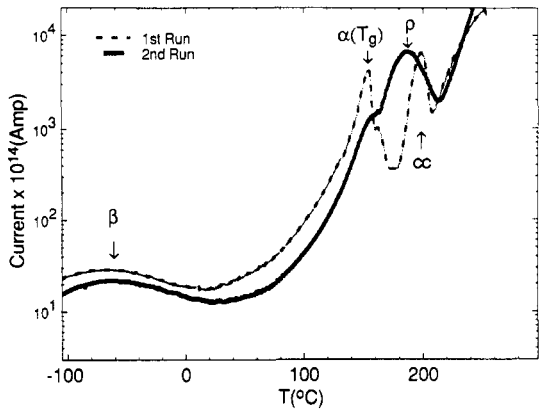

Figure 8. log plot of the global TSC depolarization current, J, vs temperature for aPEKK (dashed curve, T_p = 160) and cPEKK (solid curve, T_p = 260) at a scan rate of 7 °C/min and an excitation field strength of E = 3000 kV/m.

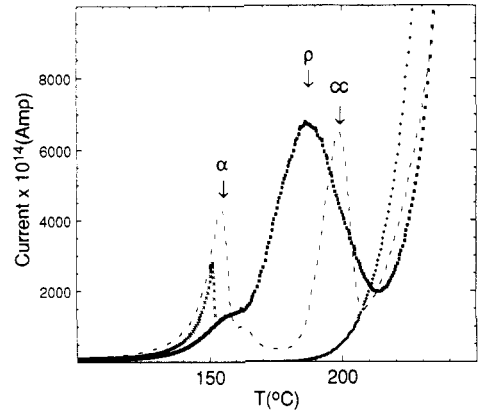

Figure 9. Linear plot of current vs temperature in the higher temperature region. Data for aPEKK were taken at polarization temperatures of T_p = 150 (×'s) and T_p = 160 (dashed line) and for cPEKK at T_p = 260 (filled squares) at a scan rate of 7 °C/min and an excitation field strength of E = 2000 kV/m. Data taken at zero excitation field strength (E = 0) shows that there is no cold-crystallization peak (cc) at 199 °C for cPEKK (crosses).

to T_g = 155 °C (428 K). The same quality of fit can be obtained by using the Vogel–Fulcher equation

$$\log (\tau/\tau_0) = A + B/(T - T_\infty) \qquad (12a)$$

where A and B are constants, and T_∞ is the temperature at which the relaxation becomes infinitely slow and is related to the WLF parameters[22] by $T_\infty = T_0 - C_2$. A three-parameter fit using eq 12 is shown as the solid curve in Figure 7, giving $\ln f_0 = -23.3$, $C_1 = 21.6$, and $C_2 = 21.2$ K. The Vogel–Fulcher fit gives T_∞ = 407 K in accord with $T_\infty = T_0 - C_2$ = 428 - 21.2 = 406.8 K calculated from the WLF parameters. The frequency range is rather limited for this analysis but we have obtained similar parameters for other high-T_g, aromatic polymers. The WLF curve does not extrapolate through the low-frequeny TSC data point in Figure 7. Saito and Nakajima[23] have presented data that also indicate that the high-frequency relaxations are not consistent with the low-frequency measurements for several polymers. In some cases, there is even an inflection in the Arrhenius plot, which indicates that E_a goes through a maximum. It is possible that physical aging during the measurement at the lower frequencies contributes to the discrepancy.

TSC Global Spectra. As discussed earlier, the TSC depolarization current is analogous to a conventional dielectric loss signal with an equivalent frequency on the order of 10^{-3} Hz.[4] The dashed curve in Figure 8 is for an amorphous sample polarized at E = 2000 kV/m from T_p = +160 down to -120 °C with the subsequent depolarization current measured upon heating from -120 to +260 °C at 7 °C/min. After the sample is heated for the first time at temperatures above ~170 °C, cold crystallization is initiated. By 260 °C the crystallization is essentially complete. The second run on this sample with T_p = 260 °C is represented by the thick curve. The β transition in the low-temperature portion of the TSC occurs at about -65 °C, independent of crystallinity, while the magnitude of the β peak is reduced by 25 ± 10% in the second cycle due to crystallinity, consistent with the dielectric results in Figure 4. The relaxation is weak with a peak current amplitude of $\sim 1 \times 10^{-13}$ A, because of the small changes in dipole moment involved in the transition. The β transition is well separated from the higher temperature transitions due to the low equivalent frequency of TSC as compared to dielectric results.

A strong α relaxation peak at 155 °C is seen for aPEKK in Figure 8, uninfluenced by the crystallization peak (cc) at 199 °C. This can be compared to dielectric results in Figure 2 where the α transition is shifted to higher temperatures and merges with the cc peak at ~200 °C. The α relaxation for cPEKK is reduced to a shoulder in Figures 8 and 9 because of the strong ρ peak at 185 °C. It has been proposed that the ρ peak is due to the release of injected space charges trapped at crystal/amorphous interfaces.[4,7] Evidence of this in terms of the intensity of the ρ transition with E will be presented later.

The magnitude of the T_g peak in Figure 9 is 3 ± 0.5 times greater for aPEKK (dashed line) than that for cPEKK (filled squares) consistent with the reduction by approximately a factor of 2 in the magnitude of the change in heat capacity from DSC (Figure 1). In other polymer samples of higher crystallinity, T_g cannot be detected by either DSC or TSC.[7] One check that is commonly performed to ensure that no significant crystallinity is induced by polarizing just above T_g is to polarize at temperatures just below T_g. The results are shown in Figure 9 for T_p = 150 °C (×'s); it is evident that only a small fraction of the T_g peak is polarized, but the magnitude of the low temperature side of the TSC is comparable, indicating that polarizing at 160 °C did not induce any detectable crystallinity.

To explain some of the higher temperature results, other aspects of the technique must be discussed. Concentrating on the dashed curve in Figure 9 for aPEKK polarized at T_p = 160 °C, only relaxations below 160 °C are excited. Thus, the peak at 199 °C for aPEKK is due to cold crystallization, which was detected by DSC (Figure 1) and dielectric analysis (first run, Figure 2), and is not a dipolar transition but is due to spontaneous reorientation into crystallites. This point can be checked by running a second scan on the fully crystallized sample at zero field strength, which results in the "base-line" curve represented by the small crosses in Figure 9. No hint of the cold-crystallization peak at 199 °C is seen because the sample has already been fully crystallized. We have found that other poly(aryl ether ketones), with a variety of crystal growth rates, show a similar behavior under conditions of E = 0. Thus, there is direct correlation with the cold crystallization peaks monitored by DSC. The base-line (E = 0) scan in Figure 9 also shows that the strong signal at T > 210 °C is due to spontaneous currents caused by conductivity.[4]

Returning to the characterization of the ρ peak in Figure 9 for cPEKK, one can determine whether a transition is dipolar[4] by plotting the peak intensity versus the field strength, E. The results are shown in Figure 10 for the α peak at 155 °C and the ρ peak at 185 °C, showing linear dependence for the α peak. Even though the intensity of

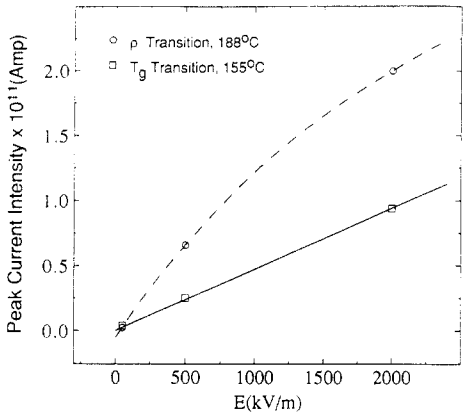

Figure 10. TSC peak current intensity vs polarization field strength, E, for the α transition at 155 °C and the ρ transition at 185 °C in cPEKK. Deviation from linearity in this data indicates that the ρ transition is nondipolar.

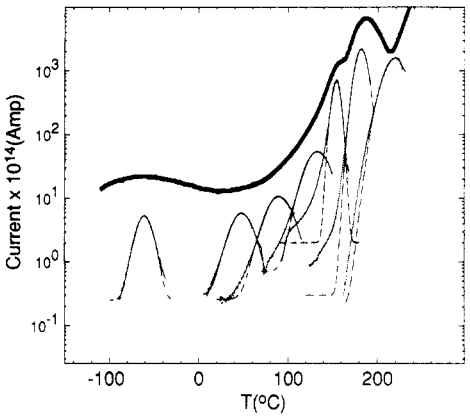

Figure 11. Global TSC spectrum and thermal cleaned spectra for cPEKK with corresponding Gaussian fits. The polarization temperatures, T_p, for the thermally cleaned spectra from left to right are −70, 40, 80, 120, 150, 180, and 210 °C. The Gaussian fits (dashed lines) are included only to indicate the range over which the Bucci plot is linear (see text).

the ρ peak is strongly dependent on E, the data deviate from linearity, which indicates that it is not due to a dipolar relaxation and is probably due to trapped space charges at crystal interfaces. Thermal cleaning of the ρ peak indicates that the relaxation dynamics are significantly different from those for the α transition, as will be discussed in the next section.

Thermal Peak Cleaning of TSC Global Spectra. It is evident that effects of crystallinity are monitored by the TSC global spectra, mainly in terms of a change in absolute intensities. One advantage of TSC over other techniques is that thermal peak cleaning (polarizing using method 2 in the Experimental Section) leads to quantitative values of E_a as a function of temperature.[6,8,11,25,26] Representative results for cPEKK are shown in Figure 11 along with the global TSC spectrum, which is the same as that presented earlier in Figure 8 for cPEKK. Gaussian fits of the experimental data in Figure 11 are given only to indicate the range over which the Bucci plot will be linear (i.e., the range characterized by a single value of E_a in terms of the Bucci plot[12]). By fractional integration of individual spectra via eq 5, Bucci plots of log τ vs $1/T$ are constructed. An example is shown for aPEKK in Figure 12 for T_p = −70 °C. The dashed line is a least-squares fit, and the slope is directly proportional to E_a, giving E_a = 13.9 kcal/mol.

Back to Figure 11, from the comparison with the Gaussian fits it is evident that a narrow distribution of activation energies governs the dynamics for the lower temperatures,

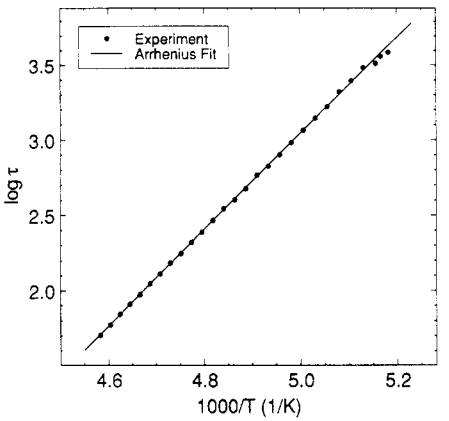

Figure 12. Bucci plot of the calculated relaxation time constant τ vs $1/T$ for a thermally cleaned TSC spectrum at T_p = −70 °C. The solid line is the least-squares fit, giving E_a = 13.9 kcal/mol.

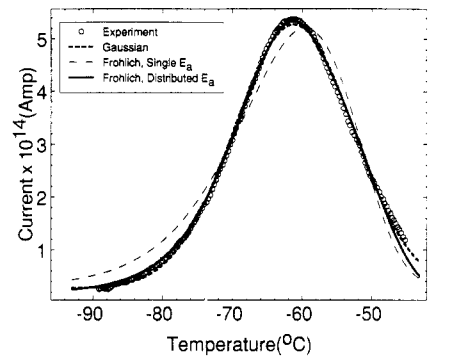

Figure 13. Current vs temperature for thermally cleaned TSC spectra for T_p = −70 °C. The Gaussian fit is only shown for the sake of comparison. Parameters obtained from the Fröhlich fit are discussed in the text and indicate a narrow distribution of activation energies.

Table I
Fröhlich and Bucci Fits of Thermally Cleaned TSC Spectra

T_p, °C	$E_{a,1}$[a]	a_1[a]	$E_{a,2}$[a]	a_2[a]	$E_{a,3}$[a]	a_3[a]	E_a[b]
−70	13.8	0.33	14.1	0.37	14.5	0.30	13.9
180	96	0.32	97	0.43	98	0.25	101.0

[a] These parameters were calculated by using the Fröhlich method where a_i is the normalized amplitude and $E_{a,i}$ is in kilocalories per mole. See text for discussion. [b] Calculated by using the Bucci method.[12]

but as one approaches T_g = 155 °C a significant low-temperature tail is seen in the experimental spectra. The log plot accentuates the deviation, and it is important to note that there is always a region spanning 1 order of magnitude in current intensity near the peak that agrees with the Gaussian curve corresponding to the linear region in the Bucci plot. The low-temperature tails for thermally cleaned TSC spectra taken just below T_g are a general feature of all other polymers studied in this lab.[24]

The alternative to the Bucci method[12] is the Fröhlich method,[11,13,17] where the current peaks are fitted directly. Solving eq 8 with a single value of E_a leads to asymmetric current peaks such as that in Figure 13 for the Fröhlich single activation energy fit of the thermally cleaned spectra at T_p = −70 °C. The agreement with experiment over the whole range is poor. Regressing on eq 11 with three discrete values of E_a results in good agreement with experiment (Fröhlich equation with a distribution in E_a). The resulting parameters are recorded in Table I, indicating that the three values of E_a obtained from the regression are spaced by only 3% and the calculated central activation energy is equal to 14.1 kcal/mol. This is in agreement with

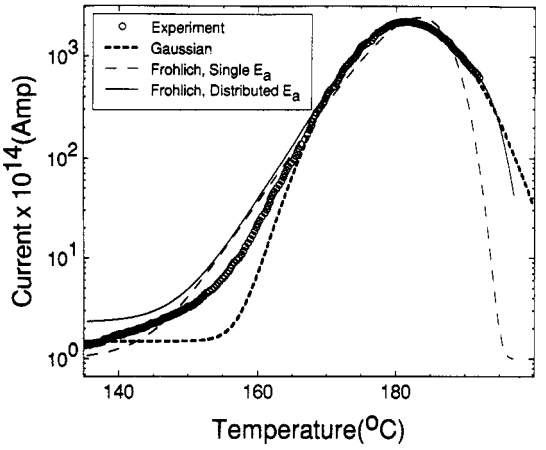

Figure 14. log plot of current vs temperature for a thermally cleaned TSC spectra taken with T_p = 180 °C. Parameters obtained from the Fröhlich fit indicate a narrow distribution of activation energies although a satisfactory fit is only obtained covering 1 order of magnitude in current intensities near the peak.

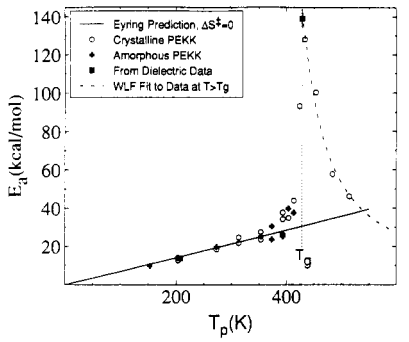

Figure 15. Apparent activation energy, E_a, vs polarization temperature in degrees Kelvin. The filled squares at 208 and 428 K are activation energies from the Arrhenius plots (Figures 6 and 7) of the dielectric loss peaks versus frequency and agree well with the TSC data obtained directly from the relaxation dynamics. The values of E_a for amorphous (dark crosses) and 27% crystalline (circles) are independent of crystallinity over the range covered. The solid curve was calculated by using Eyring's activated states theory with no adjustable parameters and $\Delta S^{\ddagger} = 0$ and $f = 10^{-3}$ Hz. The dashed curve above T_g was obtained by using the WLF expression.

the fit to the Bucci plot (Figure 12) of this same data, which gave E_a = 13.9 kcal/mol.

The thermally cleaned TSC spectrum from Figure 11, polarized at T_p = 180 °C, is replotted in Figure 14. Again, the single E_a Fröhlich fit does not agree with experiment and roughly gives E_a = 88 kcal/mol. The Gaussian fit, which has no theoretical justification, fits the data around the peak but deviates strongly in the low-temperature region. The Fröhlich fit with three values of E_a fits the data well for about 1 order of magnitude in intensity near the peak but deviates slightly on the low-temperature side. The central E_a is 97 kcal/mol in good agreement with that determined by the Bucci plot, which gave E_a = 101 kcal/mol (Table I). An extremely narrow distribution of only 1% is found for the three fitted values of E_a. Although these fits are very sensitive to small variations in E_a, we feel that the results are insensitive to the type of distribution chosen. Thus, for the rest of this report we concentrate on the mean value of E_a and how it is influenced by temperature and other material properties.

A plot of the values of E_a obtained from thermally cleaned TSC spectra is shown in Figure 15 along with predictions from Eyring's absolute rate theory for an activation entropy of zero (solid line). The activation energies from the dielectric data in Figures 6 and 7 are also plotted as the two filled squares, showing good agreement with the TSC data. The Eyring equation

$$f = kT/(2\pi h) \exp(-\Delta H^{\ddagger}/RT) \exp(\Delta S^{\ddagger}/R) \quad (13)$$

can be rearranged to give values of E_a as a function of T with no adjustable parameters, where E_a is related to $\Delta H^{\ddagger}$ by[27]

$$E_a = \Delta H^{\ddagger} + RT \quad (14)$$

The quantity RT is on the order of 0.5 kcal/mol at normal temperatures and is only a small contribution. In eqs 13 and 14, k is Boltzmann's constant, h is Plank's constant, and $\Delta H^{\ddagger}$ and $\Delta S^{\ddagger}$ are the Eyring activated states of enthalpy and entropy, respectively. The solid curve in Figure 15 was generated with the Eyring equation using $\Delta S^{\ddagger}$ = 0 and $f = 10^{-3}$ Hz. More precise values of f can be estimated by using eq 4, giving $f \sim 0.003$ Hz for the β relaxation at −65 °C and $f \sim 0.007$ Hz for the α relaxation at 155 °C. This minor correction in frequency is insignificant in Figure 15 because the logarithm of frequency is used in the calculation of E_a. The exact frequencies were used in Figures 6 and 7.

No activation energies were obtained at temperatures above ~413 K (140 °C) for amorphous PEKK in Figure 15 because of sample modification by cold crystallization. The agreement in the low-temperature region with the zero activation entropy line is a feature of all polymers studied in this lab by TSC. Starkweather[27] has shown a similar trend in dielectric and mechanical E_as for secondary relaxations for a wide range of polymers. The values of E_a are independent of crystallinity over the range covered.

Several other features deserve attention since few reports of activation energies determined above and below T_g are available. Even though the global TSC signal (Figure 8) is increasing by 2 orders of magnitude in the range 80–145 °C, the values of E_a do not change significantly and are consistent with a noncooperative type of motion as is indicated by the agreement with the Eyring equation for $\Delta S^{\ddagger} = 0$ (solid curve in Figure 15). This indicates that the large increase in current is due to an increasing population of the same type of noncooperative motions in the region below T_g. A small degree of departure from the $\Delta S^{\ddagger} = 0$ line occurs starting at about 25 °C below T_g, but this departure is close to the experimental scatter. A more significant degree of departure starting at least 50 °C below T_g has been found recently in methacrylate polymers.[24] Further analysis of the relaxation dynamics just below T_g in terms of the degree of cooperativity based on the departure of E_a[28] will be made in the future. For now it suffices to note that E_a has a maximum at T_g, and this feature could be quite useful in the analysis of complicated systems such as blends, copolymers, and other semicrystalline polymers where it is difficult to study the glass transition using conventional thermal analysis.

The data in Figure 15 indicates that there is a sharp decrease in E_a above T_g = 155 °C. Typically for relaxations at temperatures above T_g, WLF free volume analysis is used to explain the results. An effective activation energy can be defined as the tangent to the WLF curve at any given temperature (e.g., the curve in Figure 7), and the slope is given by the derivative[22]

$$E_a = R\, \partial \ln (\tau/\tau_0)/\partial(1/T) \quad (15)$$

where τ/τ_0 is given by the WLF equation (eq 12). Eval-

uating the derivative of τ/τ_0 in eq 15 gives

$$E_a = 2.303RT^2C_1C_2/[C_2 + (T - T_0)]^2 \quad (16)$$

Fitting the experimental values of E_a above T_g to eq 16 gives the dashed curve in Figure 15. The parameter T_0 is fixed at $T_0 = T_g = 428$ K, and regression gives for the other parameters; $C_1 = 13.5$ and $C_2 = 77$ K. The experimental data is of limited accuracy above T_g because the relaxation processes represent a combination of dipolar and nondipolar processes, but it is evident that the drop in E_a above T_g is qualitatively what one would expect from WLF type behavior.

Summary

TSC, dielectric, and DSC techniques were used to study molecular relaxations in semicrystalline PEKK. TSC was used to evaluate the glass transition and cold-crystallization peaks, giving results consistent with those obtained by DSC. The magnitude of the glass transition (or α relaxation) as detected by TSC and DSC is reduced by a factor of 2–3 from amorphous to semicrystalline PEKK due to the inhibiting effect of crystallites on the amorphous motions. High-frequency dielectric and TSC spectra of localized amorphous chain motions in the low-temperature β relaxation region indicate a small ($\sim$25%) reduction in peak intensity for semicrystalline PEKK consistent with a degree of crystallinity of $\sim$27%. This is consistent with the notion that the β relaxation is due to local chain motions in amorphous regions that are not influenced by neighboring crystallites.

The activation energies determined by thermal peak cleaning of the TSC spectra are consistent with those for the β and α relaxations calculated from classical Arrhenius plots of ac dielectric data. The Arrhenius plot is linear for the β transition over 8 orders of magnitude in frequency, giving a value of $E_a = 13.8 \pm 0.5$ kcal/mol. For the glass transition or α relaxation, a WLF type of deviation from simple Arrhenius behavior is found in the high-frequency dielectric results, which cover frequencies from 10^2 to 10^5 Hz and temperatures from 182 to 204 °C. When the deviation is neglected, an activation energy of 139 ± 10 kcal/mol is estimated by combining the high-frequency dielectric data with the low-frequency TSC data. This value of E_a is also in agreement with that determined directly from the thermally cleaned TSC spectra.

Thermally cleaned TSC spectra were well described by a very narrow distribution (less than 3%) of activation energies. Both the Bucci[12] and the Fröhlich[13] methods of analyzing the current spectra gave the same mean values of E_a. The values of E_a obtained as a function of the polarization temperature T_p increase continuously up to T_g and are in quantitative agreement with an Eyring model with a zero activation entropy in the range -120 °C $< T <$ 130 °C. No difference was found in E_a for amorphous and semicrystalline PEKK over the range covered. The values of E_a maximize at the glass transition and depart from the Eyring predictions, indicating a large enhancement in the cooperativity of the relaxations. This feature will be used to study and to characterize the glass transition region in complicated systems such as blends, copolymers, and other semicrystalline polymers in the future.

Acknowledgment. Discussions with R. R. Matheson and S. Mazur were most beneficial. We thank N. DiPaolo for help with the experiments and J. Dowell for performing data analysis.

References and Notes

(1) McCrum, N. G.; Read, B. E.; Williams, G. *Anelastic and Dielectric Effects in Polymeric Solids*; Wiley: New York, 1967.
(2) Boyd, R. H. *Polymer* **1985**, *26*, 323.
(3) Blundell, D. J.; Osborn, B. N. *Polymer* **1983**, *24*, 953.
(4) van Turnhout, J. *Polym. J.* **1971**, *2*, 173. van Turnhout, J. *Thermally Stimulated Discharge of Polymer Electrets*; Elsevier: Amsterdam, 1975.
(5) Hedvig, P. *Dielectric Spectroscopy of Polymers*; Hilger, A., Ed.; John Wiley and Sons: New York, 1977; p 148.
(6) Bernes, A.; Boyer, R. F.; Chatain, D.; Lacabanne, C.; Ibar, J. P. In *Order in the Amorphous State of Polymers*; Keinath, S. E., Ed.; Plenum Press: London, 1987; p 305.
(7) Belana, J.; Pujal, M.; Colomer, P.; Montserrat, S. *Polymer* **1988**, *29*, 1738.
(8) Vanderschueren, J. *J. Polym. Sci., Polym. Phys. Ed.* **1977**, *15*, 873.
(9) Gourari, A.; Bendaoud, M.; Lacabanne, C.; Boyer, R. F. *J. Polym. Sci., Polym. Phys. Ed.* **1985**, *23*, 889.
(10) Fischer, P.; Röhl, P. *J. Polym. Sci., Polym. Phys. Ed.* **1976**, *14*, 531.
(11) Fischer, P.; Röhl, P. *J. Polym. Sci., Polym. Phys. Ed.* **1976**, *14*, 543.
(12) Bucci, C.; Fieschi, R.; Guidi, G. *Phys. Rev.* **1966**, *148*, 816.
(13) Fröhlich, H. *Theory of Dielectrics*; Clarendon Press: Oxford, 1949.
(14) Chang, I. Y. *SAMPE Q.* **1988**, *19*, 29.
(15) Guerdoux, L.; Marchel, E. *Polymer* **1981**, *22*, 1199.
(16) Calame, J. P.; Fontanella, J. J.; Wintersgill, M. C.; Andeen, C. G. *J. Appl. Phys.* **1985**, *58*, 2811.
(17) Figueroa, D. R.; Fontanella, J. J.; Wintersgill, M. C.; Calame, J. P.; Andeen, C. G. *Solid State Ionics* **1988**, *28*, 1023.
(18) Matheson, R. R.; Chia, Y. T.; Avakian, P.; Gardner, K. *Polym. Prepr. (Am. Chem. Soc., Div. Polym. Chem.)* **1988**, *29* (1), 468.
(19) Avakian, P.; Gardner, K. H.; Matheson, R. R. *J. Polym. Sci., Part C: Polym. Lett.* **1990**, *28*, 243.
(20) Zoller, P.; Kehl, T. A.; Starkweather, H. A.; Jones, G. A. *J. Polym. Sci., Polym. Phys. Ed.* **1989**, *27*, 993.
(21) Lee, Y. G.; Porter, R. S. *Macromolecules* **1988**, *21*, 2770. Lee, Y. G.; Porter, R. S.; Lin, J. S. *Macromolecules* **1989**, *22*, 1756.
(22) Ferry, J. D. *Viscoelastic Properties of Polymers*, 3rd ed.; John Wiley and Sons: New York, 1980; Chapter 11.
(23) Saito, S.; Nakajima, T. *J. Appl. Polym. Sci.* **1959**, *2*, 93.
(24) Sauer, B. B.; Avakian, P., to be submitted for publication.
(25) Chatain, D.; Gautier, P.; Lacabanne, C. *J. Polym. Sci., Polym. Phys. Ed.* **1973**, *11*, 1631.
(26) Vanderschueren, J.; Linkens, A.; Haas, B.; Dellicour, E. *J. Macromol. Sci., Phys.* **1978**, *B15*, 449.
(27) Starkweather, H. W. *Macromolecules* **1981**, *14*, 1277.
(28) Gibbs, J. H.; DiMarzio, E. A. *J. Chem. Phys.* **1958**, *28*, 373.